Metformin attenuates H_2O_2-induced osteoblast apoptosis by regulating SIRT3 via the PI3K/AKT pathway

KEDA YANG, LEI PEI, SIMING ZHOU, LIN TAO and YUE ZHU

Department of Orthopedics, First Hospital of China Medical University, Shenyang, Liaoning 110001, P.R. China

Received February 22, 2021; Accepted June 11, 2021

DOI: 10.3892/etm.2021.10751

Abstract. Osteoporosis is a common metabolic disease that has a high incidence in postmenopausal women. Studies have indicated that oxidative damage plays an important role in the development of postmenopausal osteoporosis. Metformin has been showed to have the ability to relieve excessive oxidation. The aim of the present was to determine the therapeutic effect and potential mechanism of metformin in postmenopausal osteoporosis. Oxidative damage was stimulated *in vitro* by the addition of H_2O_2 to MC3T3-E1 cells and a mouse menopausal model was also constructed. Cell viability and flow cytometry experiments were performed to determine the effects of H_2O_2 and metformin treatment on apoptosis. Mitochondrial membrane potential was tested by JC-1 assays. Western blotting was used to detect the expression of mitochondrial apoptosis markers and antioxidant enzymes. Small interfering RNA was used to knockdown sirtuin3 (SIRT3), which was verified at the mRNA and protein levels. Bilateral ovariectomy was used to prepare menopausal mice, which were analyzed using micro-computed tomography. The results indicated that metformin is able to repair mitochondrial damage and inhibit the apoptosis of osteoblasts induced by H_2O_2, and also reverse bone mass loss in ovariectomized mice. Western blotting results demonstrated the involvement of SIRT3 in the production of antioxidant enzymes that are essential in protecting against mitochondrial injury. In addition, experiments with SIRT3 knockdown indicated that metformin reverses H_2O_2-induced osteoblast apoptosis by upregulating the expression of SIRT3 via the PI3K/AKT pathway. The results of the present reveal the pathogenesis of oxidative damage and the therapeutic effect of metformin in postmenopausal osteoporosis. They also suggest that SIRT3 is a potential drug target in the treatment of osteoporosis, with metformin being a candidate drug for modification and/or clinical application.

Correspondence to: Dr Yue Zhu or Dr Lin Tao, Department of Orthopedics, First Hospital of China Medical University, 155 Nanjing North Street, Shenyang, Liaoning 110001, P.R. China
E-mail: zhuyuedr@163.com
E-mail: taolindr@163.com

Abbreviations: ROS, reactive oxygen species; SIRT3, sirtuin3; SOD, superoxide dismutase; CAT, catalase

Key words: osteoporosis, metformin, mitochondria, SIRT3, PI3K/AKT

Introduction

Osteoporosis is a common metabolic disease involving reduced bone density, destruction of the bone microstructure and increased bone fragility (1). Osteoporosis is mainly caused by the inhibition of osteogenesis, which increases the risk of fracture and predominantly affects postmenopausal women (2). However, little is known about the pathogenesis of postmenopausal osteoporosis. A recent review of the literature indicated that oxidative stress is crucial to the development of osteoporosis; oxidative stress is a pathological state of the body in which reactive oxygen species (ROS) cause excessive oxidation, thereby leading to aging and disease (3). In clinical studies, the analysis of oxidation-associated serum biomarkers, including antioxidant enzymes and advanced oxidative products, has indicated that the bodies of postmenopausal women with osteoporosis are in a highly oxidative state (4). This phenomenon can be explained by the fact that estrogen is an antioxidant and, therefore, estrogen deficiency after menopause reduces the ability of the body to ameliorate high oxidative stress (5). Additionally, oxidative damage in the bone tissue has been shown to cause osteoblast apoptosis and mediate the deterioration associated with osteoporosis (6). Therefore, improvement of the oxidative state is an important means for reversing bone loss in postmenopausal women.

Metformin is a traditional hypoglycemic drug that has been used to treat tumors and delay aging and has exhibited promising effects (7-9). Metformin has also exhibited a therapeutic effect in diabetes-associated osteoporosis, mediated by the amelioration of the hyperglycemic microenvironment (10). However, the therapeutic effect was only attributed to mitigation of the effects of high glucose. The use of metformin in postmenopausal osteoporosis has not yet been investigated. Since metformin is able to improve the oxidative state in numerous diseases, including diabetes and fatty liver (11,12), the aim of the present study was to determine the role of metformin in the treatment of postmenopausal osteoporosis.

Mitochondria are the main organelles involved in the maintenance of redox balance in a cell (13). Most antioxidant enzymes are able to eliminate peroxide and prevent the

release of ROS in mitochondria. During the development of osteoporosis, the dysfunction of mitochondria in osteoblasts leads to the excessive generation of ROS, which cause damage to other organelles and induce apoptosis (14). Sirtuin3 (SIRT3) is an important deacetylating enzyme and an upstream regulator of the activity of numerous metabolic enzymes and mitochondrial metabolism (15-17). Increasing the expression of SIRT3 is expected to contribute to the repair of mitochondrial damage in osteoblasts and attenuate the loss of bone mass.

The present study investigated the hypothesis that metformin can improve the activity of antioxidant enzymes and attenuate the osteoblast apoptosis induced by H_2O_2 by upregulating SIRT3 expression via the PI3K/AKT pathway. The role of oxidative damage in the development of postmenopausal osteoporosis was evaluated, to provide a potential target for the treatment of osteoporosis. The direct effect of metformin on osteoblasts and the therapeutic effect on an animal model of postmenopausal osteoporosis were also revealed. The findings may contribute to our understanding of the pathogenesis of postmenopausal osteoporosis and suggest novel therapeutic targets.

Materials and methods

Reagents and cell culture. MC3T3-E1 cells were purchased from the Cell Bank of Type Culture Collection of the Chinese Academy of Sciences. Metformin was purchased from Dalian Meilun Biotechnology Co., Ltd. Antibodies against SIRT3 (1:1,000; cat. no. ab246522), catalase (CAT) (1:2,000; cat. no. ab209211), superoxide dismutase 1 (SOD 1) (1:2,000; cat. no. ab51254), COX IV (1:1,000; cat. no. ab16056) cleaved caspase-3 (1:1,000; cat. no. ab214430), caspase-3 (1:1,000; cat. no. ab184787) and Bcl-2 (1:1,000; cat. no. ab182858) were obtained from Abcam. Bax (1:1,000; cat. no. 60267-1-Ig), cytochrome *c* (1:1,000; cat no: 66264-1-Ig) and β-actin (1:2,000; cat. no. 66009-1-Ig) antibodies and horseradish peroxidase-conjugated anti-mouse and anti-rat secondary antibodies (both 1:2,000; cat. nos. SA00001-1 and SA00001-15, respectively) were obtained from ProteinTech Group, Inc. In addition, antibodies against PI3K (1:1,000; cat. no. 4257), phosphorylated (p-)PI3K (1:1,000; cat. no. 4228), AKT (1:1,000; cat. no. 4691) and p-AKT (1:1,000; cat. no. 4060) were purchased from Cell Signaling Technology, Inc.

MC3T3-E1 cells were cultured in α-Minimal Essential Medium (HyClone; Cytiva) supplemented with 10% fetal bovine serum (HyClone; Cytiva), 100 U/ml streptomycin sulfate and 100 mg/ml penicillin. Cells were grown in a humidified incubator with 5% CO_2 at 37˚C (18). H_2O_2 was added to the medium to induce an oxidative damage model at a concentration gradient of 0.1, 0.2 and 0.3 mM. Then, various concentrations of metformin (0.05, 0.1, 0.2, 0.3 and 0.4 mM) were added with 0.2 mM H_2O_2 to determine the optimal concentration based on cell apoptosis measured by flow cytometry.

Cell viability assay. Cell Counting Kit-8 (CCK-8) colorimetric assay (Dojindo Molecular Technologies, Inc.) was used to measure the viability of the cells after metformin treatment to assess drug cytotoxicity. MC3T3-E1 cells were plated into 96-well plates at $5x10^3$ cells/well in 100 μl medium/well. Cells were treated with the aforementioned concentrations of H_2O_2 for 6 h and metformin for 24, 48 and 72 h separately in a 37˚C humidified incubator. CCK-8 solution was added at 10 μl/well, and the cells were incubated in a humidified incubator for another 1 h. Cell viability was then determined based on the absorbance at 450 nm.

Apoptosis assay by flow cytometry. Various concentrations of metformin (0.05, 0.1, 0.2, and 0.3 mM) were added with 0.2 mM H_2O_2 to 6-well plates seeded with $1.2x10^6$ MC3T3-E1 cells and incubated at 37˚C for 6 h. The cells were then harvested, resuspended in binding buffer and stained with FITC-Annexin V/propidium iodide for 15 min using Annexin V-FITC kit (Beyotime Institute of Biotechnology), in the dark at room temperature (19). Apoptosis was detected using a FACScan flow cytometer (BD Biosciences) and analyzed with CytExpert 2.3 (Beckman Coulter, Inc.).

Western blotting. To isolate the proteins, the culture solution was decanted from the treated cells and phosphate-buffered saline (PBS) was used to wash the cells three times. The Petri dishes were placed on ice after decanting the PBS. Radioimmunoprecipitation assay buffer (Beyotime Institute of Biotechnology) and phenylmethylsulfonyl fluoride were mixed at a ratio of 1:1,000 and 100 μl mixture was incubated with the cells on ice for 30 min. The extract was then transferred to 1.5-ml centrifuge tubes and centrifuged at 12,000 x g and 4˚C for 5 min. The supernatant containing total protein was collected in a new 1.5-ml centrifuge tube and stored at -20˚C. Bone tissue protein extraction kit (Beijing Biolab Technology Co., Ltd.) was used to extract protein from mouse bone tissue. Bone tissue was fully soaked in saline and washed with distilled water to remove blood and red blood cells. Bone tissue was cut into small pieces, weighed, placed in a mortar filled with liquid nitrogen and ground into powder. The powder was transferred into a centrifuge tube. A total of 200-300 μl protein extraction reagent per 100 mg bone tissue was added and mixed for 30 min on ice. Then, the mixture was centrifuged at 12,000 x g and 4˚C for 15 min. Supernatant was collected in a new 1.5-ml centrifuge tube and stored at -20˚C. BCA assay kit (Beyotime Institute of Biotechnology) was used to measure protein concentration. Then, 50 μg protein/lane was resolved by 10 and 12% SDS-PAGE and transferred to polyvinylidene difluoride membranes. The membranes were blocked with 5% skimmed milk for 1.5 h at room temperature. After washing with 1% TBST, the membranes were incubated with the aforementioned primary antibodies at 4˚C overnight and secondary antibody at 4˚C for 1.5 h on the next day. After washing thoroughly, the protein bands were coated with an enhanced chemiluminescence system (Analytik Jena AG) and visualized using a chemiluminescence imaging system (Analytik Jena AG) (20). Protein levels were normalized to β-actin (molecular weight, 43 kDa). Finally, ImageJ v1.8.0 software (National Institutes of Health) was used to calculate the optical density and relative protein expression levels. For the detection of cytochrome *c*, mitochondria were separated using a Cell Mitochondria Isolation kit (Beyotime Institute of Biotechnology) and the expression levels of cytochrome *c* in the mitochondria and cytosol were analyzed.

Detection of mitochondrial membrane potential using JC-1. A Mitochondrial Membrane Potential Assay kit with JC-1 (Beyotime Institute of Biotechnology) was used to evaluate the mitochondrial membrane potential of the MC3T3-E1 cells after the aforementioned treatments. The cells were suspended in JC-1 staining working solution for 30 min in a humidified incubator at 37˚C and then washed with JC-1 buffer solution three times. Relative changes were detected by flow cytometry (CytoFLEX System B3-R3-V3) and analyzed with CytExpert 2.3 (both Beckman Coulter, Inc.). Absolute changes were detected using a multifunctional microplate reader. JC-1 fluorescence was measured at excitation/emission wavelengths at 585/590 (red) and 510/527 nm (green). The red/green ratios were calculated to indicate the mitochondrial membrane potential.

Reverse transcription-quantitative PCR (RT-qPCR) assay. A miRNeasy RNA mini kit (Qiagen, Inc.) was used to extract total RNA from cells. Then, GoScript™ Reverse Transcription mix, Oligo(dT) (Promega Corporation) were used to synthesize cDNA from the RNA according to the manufacturer's protocol. qPCR was performed using GoTaq® qPCR Master Mix (Promega Corporation). The thermocycling conditions were as follows: Denaturation at 95 ˚C for 15 sec, annealing at 60˚C for 20 sec and extension at 72˚C for 1 min, for 40 cycles. The data were collected using a Roche Light Cycler® 480 instrument II (Roche Diagnostics). mRNA expression was calculated using the $2^{-\Delta\Delta Cq}$ method (21). Primers for the qPCR analysis of SIRT3 and the reference gene b-actin are listed in Table I.

Cell transfection. SIRT3-small interfering RNAs (siRNAs) were designed and synthesized by SynBio-Tech (Suzhou) Co., Ltd. The inhibition efficiencies of three different siRNA sequences were determined, and SIRT3-si-2 with the highest inhibition efficiency (73.4%) was used in the experiments. The siRNA sequences are presented in Table II. A total of 50 nM siRNA duplexes were transfected into MC3T3-E1 cells for 48 h using Lipofectamine™ 3000 reagent (Invitrogen; Thermo Fisher Scientific, Inc.) according to the manufacturer's instructions. Untreated cells were used as a control to verify the effect of cell transfection. The cells were used in the experiments 2 days after transfection at 37˚C.

Animal experiments. A total of 15 C57BL/6J female mice (8 weeks, 20-25 g) were obtained and housed in the Department of Laboratory Animal Science of China Medical University. The laboratory environment was maintained at a temperature of 20-26˚C, 40-70% relative humidity, ≤14 mg/m^3 ammonia concentration, ≤60 dB noise and a 12-h alternating light/dark cycle with *ad libitum* access to food and drinking water. All animals were adapted to the environment for 2 weeks before the experiments. The mice were randomly divided into three groups (n=5/group); two groups (OVX) were selected for ovariectomy treatment, and the remaining group underwent a sham surgery (the epidermis and peritoneum were cut, then sutured). The mice in the OVX groups were subjected to bilateral ovariectomy under 1.4-1.5% isoflurane inhalation anesthesia with oxygen. Metformin was directly dissolved in 0.9% normal saline, and mice in one of the OVX groups (OVX + Met) were injected with metformin (100 mg/kg/day) intragastrically, starting 3 days after surgery. The mice in the OVX and sham groups were treated with normal saline in a similar manner. After treatment for 8 weeks, all mice were sacrificed via exsanguination under isoflurane anesthesia. Bilateral femurs and tibias were harvested for imaging and protein extraction. All animal experiments were performed according to laboratory and animal welfare guidelines and were approved by the Animal Ethics Committee of the First Affiliated Hospital of China Medical University (approval no. 2019014).

Microcomputed tomography (micro-CT). The femurs were evaluated by microcomputed tomography (Skyscan 1276 Micro-CT; Bruker Corporation). X-ray images at each angle were reconstructed into a 3-dimensional image analyzed by the CT-analyser software CTAn 1.19.11.1 (Bruker Corporation). The following variables were determined: Bone volume/tissue volume ratio (BV/TV), bone surface/bone volume ratio (BS/BV), trabecular separation (Tb.Sp) and trabecular thickness (Tb.Th).

Statistical analysis. Student's t-tests and one-way ANOVA followed by Tukey's post hoc tests were used for the statistical analysis. Experiments were performed with three replicates and were analyzed using SPSS 19.0 software (IBM Corp.). $P<0.05$ was considered statistically significant.

Results

Metformin inhibits apoptosis induced by H_2O_2 in MC3T3-E1 cells. The effect of metformin on osteoblasts under H_2O_2-induced highly oxidative conditions was evaluated. A CCK-8 cell viability assay was performed to investigate the effects of different concentrations of H_2O_2 on cell viability and thereby determine the appropriate concentration for use in subsequent experiments. H_2O_2 concentrations of 0.1, 0.2 and 0.3 mM were used to treat cultured osteoblasts for 6 h. The results revealed a weak effect of 0.1 mM, intermediate effect of 0.2 mM and strong effect of 0.3 mM (Fig. 1A). As the loss of viability at 0.3 mM was considered too high and different from *in vivo* conditions, the 0.2-mM concentration was deemed appropriate and selected for further experiments. Additionally, co-treatment of the cells with 0.2 mM H_2O_2 and various concentrations of metformin (0.05, 0.1, 0.2, 0.3 and 0.4 mM) indicated that only the 0.4-mM concentration had a negative effect on cell proliferation (Fig. 1B). Flow cytometry was used to evaluate the alleviating effect of metformin at concentrations of 0.05-0.3 on 0.2 mM H_2O_2 induced osteoblast apoptosis. All metformin concentrations inhibited apoptosis, and treatment with 0.2 mM metformin exhibited the strongest ability to attenuate apoptosis (Fig. 1C and D). Therefore, this concentration of metformin was used in subsequent experiments.

Metformin reverses osteoblast apoptosis induced by H_2O_2 via the mitochondrial pathway. The western blot analysis of proteins involved in the mitochondrial apoptotic pathway indicated that the levels of Bax, cleaved caspase-3 and cytosolic cytochrome *c* were increased, and the level of Bcl-2

Table I. Primers for quantitative polymerase chain reaction.

Name	Forward (5'-3')	Reverse (5'-3')
SIRT3	ATCCCGGACTTCAGATCCCC	CAACATGAAAAAGGGCTTGGG
β-actin	GGCTGTATTCCCCTCCATCG	CCAGTTGGTAACAATGCCATGT

SIRT3, sirtuin3.

Table II. RNA interference sequences used for transfection.

Name	Forward (5'-3')	Reverse (5'-3')
SIRT3-si-1	CCCUGAACCCAUCUUUGAAdTdT	UUCAAAGAUGGCUUCAGGGdTdT
SIRT3-si-2	GCAAGGUUCCUACUCCAUAdTdT	UAUGGAGUAGGAACCUUGCdTdT
SIRT3-si-3	GGAUCUUACGCAGCGGGAAdTdT	UUCCCGCUGCAUAAGAUCCdTdT

SIRT3, sirtuin3; si, small interfering RNA.

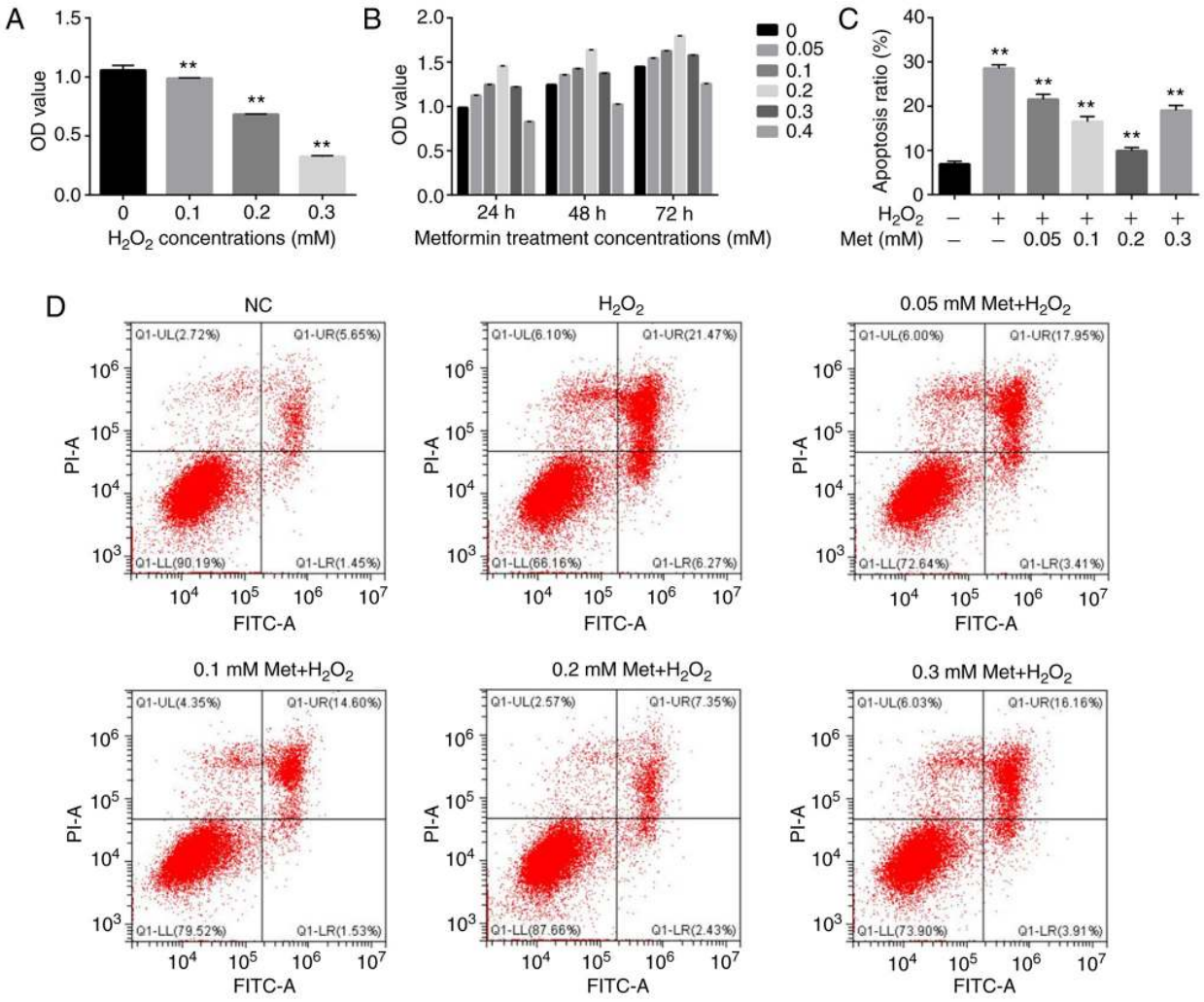

Figure 1. Met inhibits apoptosis induced by H_2O_2 in MC3T3-E1 cells. (A) Cells were treated with H_2O_2 for 6 h, and a suitable concentration of H_2O_2 was selected based on cell viability measured by CCK-8 assay. (B) CCK-8 assay results for evaluation of the effect of Met on the proliferation of MC3T3-E1 cells. (C) Apoptosis rate of MC3T3-E1 cells treated with 0.2 mM H_2O_2 with or without different concentrations of Met to select the optimum Met concentration, as determined by flow cytometry. (D) Representative flow cytometry plots. Experiments were performed in triplicate. Data are presented as the mean ± SD. **P<0.01 vs. control cells analyzed using ANOVA followed by Tukey's post hoc tests. CCK-8, Cell Counting Kit-8; Met, metformin; NC, negative control; FITC-A, FITC-Annexin V; OD, optical density.

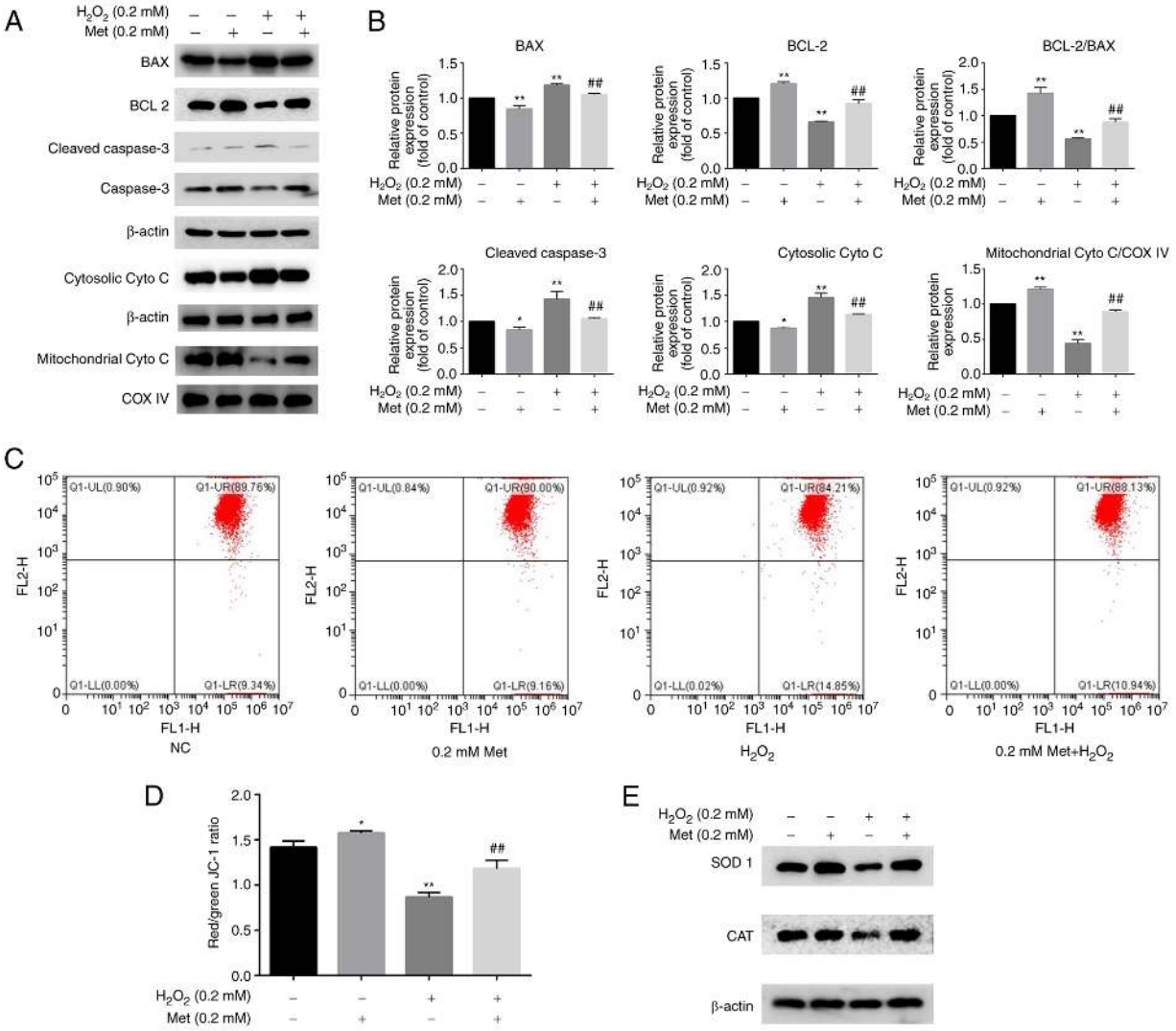

Figure 2. Met reverses osteoblast apoptosis induced by H_2O_2 via the mitochondrial pathway. (A) Marker proteins in the mitochondrial apoptosis pathway were detected by western blotting in MC3T3-E1 cells treated with H_2O_2 and/or Met. Representative blots are shown. (B) Expression levels of the proteins in (A) relative to those in the control group. (C) Qualitative changes of mitochondrial membrane potential were detected by flow cytometry. (D) Quantitative changes of mitochondrial membrane potential were detected using a full-wavelength multifunctional microplate reader. (E) Protein expression of anti-oxidase SOD 1 and CAT detected by western blotting, showing that Met improves the expression of antioxidant enzymes. Experiments were performed in triplicate. Data are presented as the mean ± SD. *P<0.05, **P<0.01 vs. control cells and $^{\#\#}$P<0.01 vs. H_2O_2 treatment alone analyzed using ANOVA followed by Tukey's post hoc tests. Met, metformin; cyto *c*, cytochrome *c*; COX IV, cyto *c* oxidase subunit 4; SOD 1, superoxide dismutase 1; CAT, catalase; FL1, green JC-1 fluorescence (monomer); FL2, red JC-1 fluorescence (aggregates).

and mitochondrial cytochrome *c* were decreased following induction with 0.2 mM H_2O_2; these changes were attenuated by treatment with 0.2 mM metformin (Fig. 2A and B). JC-1 is a fluorescent probe used to detect the mitochondrial membrane potential. A reduction in mitochondrial membrane potential is an important event in the early stage of apoptosis (22). Changes in the mitochondrial membrane potential were detected by a mitochondrial membrane potential assay using JC-1. The results indicated that metformin inhibited H_2O_2-induced mitochondrial injury (Fig. 2C and D). Additionally, the expression levels of SOD 1 and CAT, which are important regulators of ROS production in mitochondria, were determined. The expression levels of these proteins were decreased after treatment with H_2O_2 and increased by metformin co-treatment (Fig. 2E). These results suggest that H_2O_2 induces apoptosis via the mitochondrial pathway by changing the mitochondrial membrane potential and causing an imbalance in ROS, and these effects are reversed by metformin.

Metformin ameliorates osteoblast apoptosis induced by H_2O_2 by upregulating SIRT3 expression via the PI3K/AKT pathway. To determine the role of SIRT3 in the reversal of H_2O_2-induced apoptosis by metformin, the SIRT3 gene was knocked down by transfection of the cells with SIRT3-siRNA (Fig. 3A). The data in Fig. 3B and C indicate that in cells treated with H_2O_2 and metformin, the targeted knockdown of SIRT3 attenuated the metformin-induced reduction in apoptosis. Marker proteins of the mitochondrial apoptosis pathway were detected by western blotting. The levels of Bax, cleaved caspase-3 and cytosolic cytochrome *c* increased and the level of Bcl-2 was decreased in the H_2O_2 and metformin-treated cells with SIRT3 knockdown compared with those without SIRT3 knockdown (Fig. 3D). Additionally, the direct effect of metformin on the expression

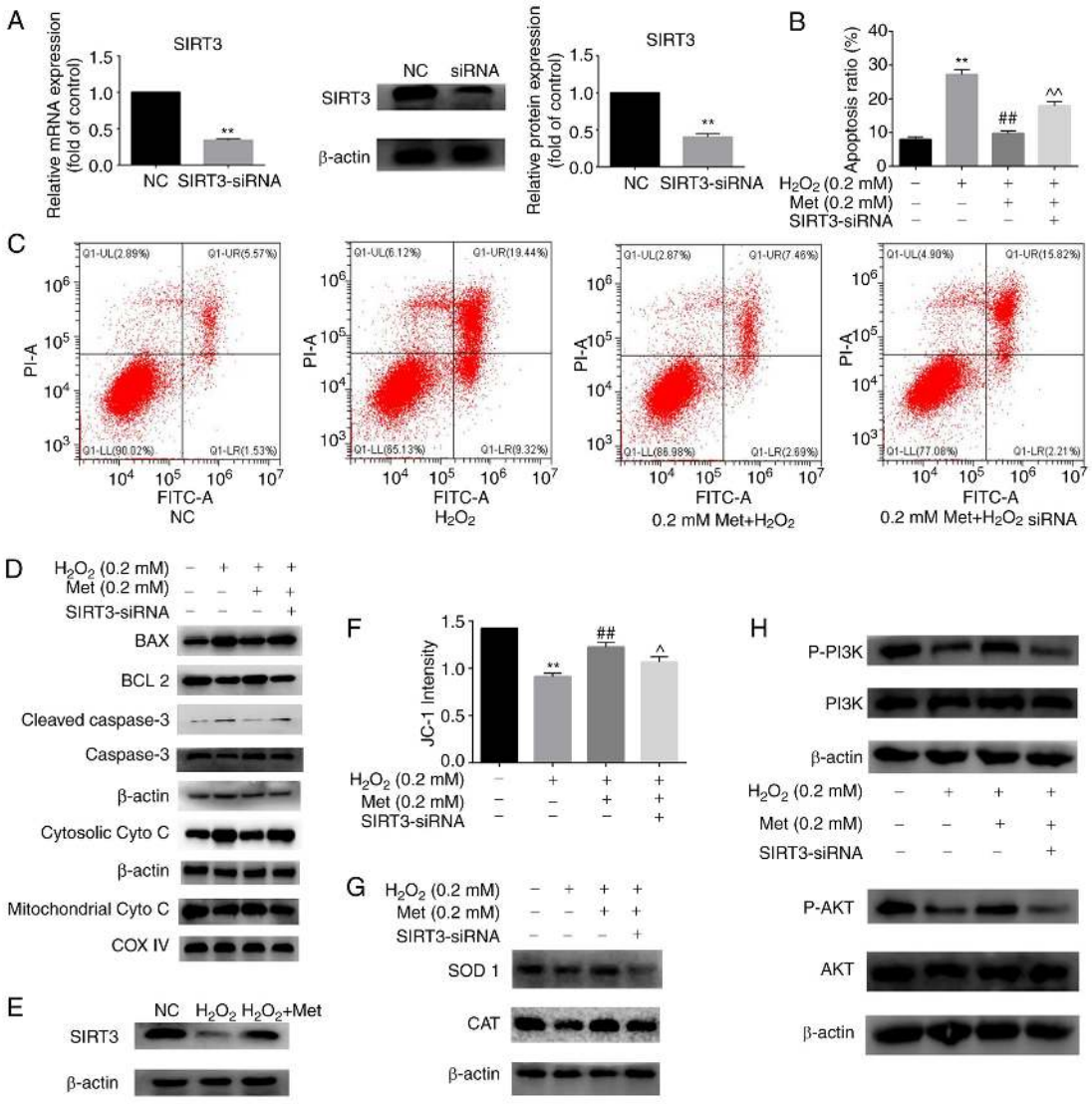

Figure 3. Met ameliorates osteoblast apoptosis induced by H_2O_2 by upregulating SIRT3 expression via the PI3K/AKT pathway. (A) Transfection efficiency of SIRT3 knockdown was detected at the mRNA and protein levels. (B) Apoptosis rate of MC3T3-E1 cells after incubation for 6 h in the control, H_2O_2, H_2O_2 + 0.2 mM Met and H_2O_2 + 0.2 mM Met + SIRT3-siRNA group. (C) Detection of cell apoptosis in the four groups by flow cytometry. (D) Marker proteins in the mitochondrial apoptosis pathway were detected by western blotting in the four groups. (E) Effect of Met on the protein expression of SIRT3. (F) Quantitative changes in mitochondrial membrane potential were detected using a full-wavelength multifunctional microplate reader. (G) Protein expression of the antioxidant enzymes SOD 1 and CAT tested by western blotting shows that SIRT3-siRNA interferes with the anti-oxidative effect of Met. (H) Western blotting of proteins in the PI3K-AKT pathway shows the involvement of this pathway in the SIRT3-mediated protective effect of Met against osteoblast apoptosis. Experiments were performed in triplicate. Data are presented as the mean ± SD. **P<0.01 vs. control cells, $^{\#\#}$P<0.01 vs. H_2O_2 alone and $^{\wedge}$P<0.05 and $^{\wedge\wedge}$P<0.01 vs. H_2O_2 + Met analyzed using ANOVA followed by Tukey's post hoc tests. Met, metformin; SIRT3, sirtuin3; siRNA, small interfering RNA; NC, negative control; cyto *c*, cytochrome *c*; COX IV, cyto *c* oxidase subunit 4; SOD 1, superoxide dismutase 1; CAT, catalase; p-, phosphorylated.

of SIRT3 was detected, and the results indicated that metformin attenuated the H_2O_2-induced reduction in SIRT3 expression in osteoblasts (Fig. 3E). The mitochondrial membrane potential was also measured using a microplate reader, and the results show that the ability of metformin to inhibit the H_2O_2-induced change in mitochondrial membrane potential was attenuated by SIRT3 knockdown, indicating that SIRT3 is involved in the mechanism by which metformin protects the mitochondria (Fig. 3F). In the H_2O_2 and metformin-treated cells, the protein levels of SOD 1 and CAT were decreased following SIRT3 knockdown (Fig. 3G), indicating that the oxidative state and ROS levels were increased. The PI3K/AKT signaling pathway is closely associated with cell proliferation, differentiation and apoptosis (23). In order to investigate whether this pathway is involved in the protective mechanism of metformin against H_2O_2-induced osteoblast apoptosis, the levels of proteins in the PI3K/AKT pathway were measured. The results in Fig. 3H show that the activation of PI3K/AKT was inhibited in osteoblasts under apoptosis-inducing conditions and preserved with metformin co-treatment. When SIRT3 was silenced, the preventive effect of metformin was suppressed. These results suggest that metformin protects the mitochondria and prevents the H_2O_2-induced apoptosis of MC3T3-E1 cells by enhancing SIRT3 expression via the PI3K/AKT signaling pathway.

Metformin ameliorates bone loss in OVX mice. To verify whether metformin can prevent the development of osteoporosis in postmenopausal mice, a menopausal mouse model

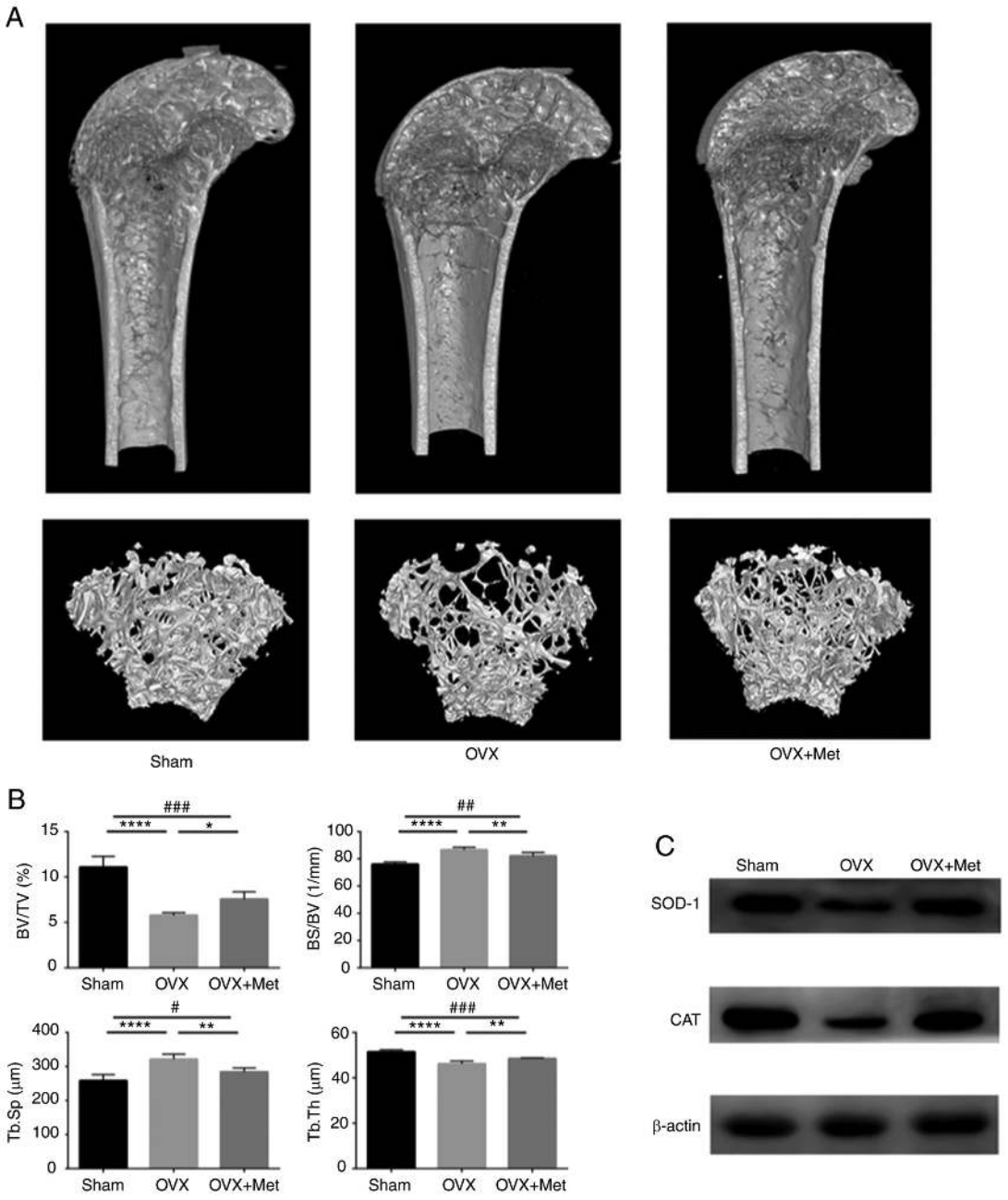

Figure 4. Met attenuates bone loss in ovariectomized mice. (A) 3-Dimensional reconstruction of the micro-CT images of femurs extracted from mice from the sham, OVX and OVX + Met groups. (B) BV/TV, BS/BV, Tb.Th and Tb.Sp values determined by micro-CT. (C) Protein level of the antioxidant enzymes SOD 1 and CAT in bone tissue extracted from femurs. Data are presented as the mean ± SD (n=5 specimens/group). *P<0.05, **P<0.01 and ****P<0.0001 vs. OVX, and $^{\#}$P<0.05, $^{\#\#}$P<0.01 and $^{\#\#\#}$P<0.001 sham vs. OVX + Met analyzed using ANOVA followed by Tukey's post hoc tests. Met, metformin; BV/TV, bone volume/tissue volume (percentage bone volume); BS/BV, bone surface/bone volume (bone surface/volume ratio; Tb.Th, trabecular thickness; Tb.Sp trabecular separation; CT, computed tomography; OVX, ovariectomy; SOD 1, superoxide dismutase 1; CAT, catalase.

was generated by bilateral ovariectomy. After observation for 3 days, the ovariectomized mice were divided into two groups with or without intragastric metformin. A sham group was also established to verify the reliability of the model. The bone mass was assessed and microstructure was observed by micro-CT analysis. As shown in Fig. 4A, the trabecular bone mass was lower in the OVX group compared with the sham group, and the phenomenon was attenuated by metformin feeding. The data obtained by micro-CT scanning showed that Tb.Th and the BV/TV ratio were decreased in OVX mice compared with those in the sham group but were increased in the OVX + Met group compared with the OVX group. In addition, Tb.Sp and the BS/BV ratio were higher in the OVX group than those in the sham group and were decreased after metformin feeding (Fig. 4B). All the data indicate that bilateral ovariectomy led to a reduction in the bone mass of female mice and that intragastric metformin can prevent this deterioration.

To evaluate the oxidative level in the bone tissue of the mice, the protein levels of SOD 1 and CAT were assayed by western blotting. The results indicate that SOD 1 and CAT expression levels were lower in OVX mice compared with those in the sham group and were increased after treatment with metformin (Fig. 4C). These changes indicate that

estrogen deficiency disrupts the redox balance and induces a high-oxidation state of the bone, which may lead to the apoptosis of osteoblasts and development of osteoporosis.

Discussion

At present, the treatment of osteoporosis is focused on direct action on osteoblasts and osteoclasts; for example, teriparatide promotes bone formation and bisphosphonates inhibit bone resorption. However, the condition of the patients remains unstable and is recurrent following drug withdrawal (24,25). The targeted treatment of osteoblasts or osteoclasts is limited, and the systemic regulation of osteoporosis is the focus of further studies. Oxidative stress is regarded as the main factor leading to body aging and organ damage (26-28). Studies have indicated that postmenopausal women generally have reduced antioxidant capacity and are in a highly oxidized state (29,30). The present study is consistent with this; OVX mice were established and shown to have reduced bone levels of antioxidative enzymes. Following treatment with metformin, the results indicated that the bone mass increased and the oxidative state of bone tissue was improved after the treatment.

The present study also investigated the effect and mechanism of action of metformin on oxidative modulation in osteoblasts. Oxidative damage is caused by the excessive generation of ROS that attack cell membranes and destroy protein structures and genetic materials (31). Under physiological conditions, ROS are produced in the mitochondria and are partially eliminated by antioxidants, such as SOD and CAT, to maintain a dynamic balance. When excessive amounts of free radicals are produced and the antioxidant function is decreased, the ability of the body to eliminate and self-repair may be exceeded; therefore, the release of copious quantities of free radicals induces apoptosis (32). Thus, H_2O_2 was used in the present study to mimic the hyperoxidative state in postmenopausal osteoporosis and induce osteoblast apoptosis. The results indicated that the H_2O_2-induced changes in apoptosis and antioxidant levels were reversed by metformin treatment. Thus, metformin may prevent H_2O_2-induced osteoblast apoptosis by improving mitochondrial function.

Subsequently, the mechanism by which metformin regulates mitochondrial function was investigated. The SIRT protein family is important for the regulation of metabolism and aging (33). SIRT3 is associated with mitochondrial biogenesis and regulates the acetylation levels of metabolic enzymes in the mitochondria (34,35). SIRT3 has been demonstrated to increase the expression of CAT and SOD via the upregulation of forkhead box O3a in the nucleus (36,37). The excessive production of ROS can induce p53-mediated apoptosis (38). However, enhancing the expression of SIRT3 can eliminate ROS, while a deficiency in SIRT3 leads to oxidative damage and accelerates aging (39,40). SIRT3 weakens the binding between p53 and Bcl-2 associated athanogene 2 to activate the Bcl-2-mediated apoptosis-inhibiting pathway (41). A reduction in the Bax/Bcl-2 ratio inhibits the expression of cytochrome *c*, thereby reducing the activation of caspase-3 (42). Additionally, studies have shown that SIRT3 expression is decreased in an oxidative damage model of osteoblasts induced by H_2O_2 and in a rat model of postmenopausal osteoporosis (43,44). This evidence indicates that SIRT3 may play an important role in the metformin-dependent reversal of the apoptosis of osteoblasts caused by oxidative damage. In the present study, transfection technology was used to knockdown the expression of SIRT3, and the data indicate that the therapeutic effect of metformin was inhibited by the knockdown of SIRT3. These results indirectly indicate that metformin reverses the mitochondrial injury caused by H_2O_2 by upregulating the expression of SIRT3. Additionally, the PI3K/AKT pathway makes an important contribution to mitochondrial apoptosis. In the present study, the results also indicated that the SIRT3-mediated protective effect of metformin against osteoblast apoptosis was mediated via the PI3K/AKT signaling pathway. In previous studies, attention has focused on how metformin inhibits apoptosis associated with oxidative damage (45,46). However, the present study proceeded from the effect of metformin on apoptosis, and focused on the protection of mitochondrial function and regulation of antioxidant enzymes by metformin.

Due to a limited understanding of the pathogenesis of osteoporosis, the current drugs for treating this condition are mainly aimed at the inhibition of osteoclasts (47,48). However, a simple decline in the effect of osteoclasts can only delay the deterioration induced by osteoporosis, and a decline in osteogenesis will continue to cause continuous bone mass loss concomitant to aging. Inhibition of the apoptosis of osteoblasts is an effective means for the treatment of osteoporosis. The present study demonstrates that oxidative damage is involved in the pathogenesis of postmenopausal osteoporosis, and metformin is an effective drug therapy. Additionally, the study provides a potential target for treatment, SIRT3, thus contributing to drug design and development. Further clarification of the role of oxidative damage in the development of osteoporosis and the effect of metformin on osteoclasts will be the focus of future research.

Acknowledgements

Not applicable.

Funding

The study was supported by the National Natural Science Foundation of China (grant no. 81472044), Construction of Clinical Medical Research Center of Orthopaedics and Sports Rehabilitation Diseases in Liaoning Province (grant no. 2019416030).

Availability of data and materials

The datasets used and/or analyzed during the current study are available from the corresponding author on reasonable request.

Authors' contributions

KY was responsible for annotating and maintaining research data, formal analysis and writing the original draft of the manuscript. LP contributed to methodology, and software support for data acquisition and analysis. SZ performed the

experiments. LT was responsible for conceptualization and validation. YZ was involved in conceptualization, funding acquisition, project administration, providing resources, and reviewing and editing the manuscript. All authors read and approved the final manuscript. KY and YZ confirm the authenticity of all the raw data.

Ethics approval and consent to participate

All animal experiments were approved by the Animal Ethics Committee of the First Affiliated Hospital of China Medical University (no. 2019014).

Patient consent for publication

Not applicable.

Competing interests

The authors declare that they have no competing interests.

References

1. Glaser DL and Kaplan FS: Osteoporosis. Definition and clinical presentation. Spine (Phila Pa 1976) 22 (Suppl 24): S12-S16, 1997.
2. Rodan GA and Martin TJ: Therapeutic approaches to bone diseases. Science 289: 1508-1514, 2000.
3. Sies H and Jones DP: Reactive oxygen species (ROS) as pleiotropic physiological signalling agents. Nat Rev Mol Cell Biol 21: 363-383, 2020.
4. Zhou Q, Zhu L, Zhang D, Li N, Li Q, Dai P, Mao Y, Li X, Ma J and Huang S: Oxidative stress-related biomarkers in postmenopausal osteoporosis: A systematic review and meta-analyses. Dis Markers 2016: 7067984, 2016.
5. Guetta V, Quyyumi AA, Prasad A, Panza JA, Waclawiw M and Cannon RO III: The role of nitric oxide in coronary vascular effects of estrogen in postmenopausal women. Circulation 96: 2795-2801, 1997.
6. Nollet M, Santucci-Darmanin S, Breuil V, Al-Sahlanee R, Cros C, Topi M, Momier D, Samson M, Pagnotta S, Cailleteau L, *et al*: Autophagy in osteoblasts is involved in mineralization and bone homeostasis. Autophagy 10: 1965-1977, 2014.
7. Dahmani Z, Addou-Klouche L, Gizard F, Dahou S, Messaoud A, Chahinez Djebri N, Benaissti MI, Mostefaoui M, Terbeche H, Nouari W, *et al*: Metformin partially reverses the inhibitory effect of co-culture with ER-/PR-/HER2+ breast cancer cells on biomarkers of monocyte antitumor activity. PLoS One 15: e0240982, 2020.
8. Kim Y, Vagia E, Viveiros P, Kang CY, Lee JY, Gim G, Cho S, Choi H, Kim L, Park I, *et al*: Overcoming acquired resistance to PD-1 inhibitor with the addition of metformin in small cell lung cancer (SCLC). Cancer Immunol Immunother 70: 961-965, 2021.
9. Pryor R, Norvaisas P, Marinos G, Best L, Thingholm LB, Quintaneiro LM, De Haes W, Esser D, Waschina S, Lujan C, *et al*: Host-Microbe-Drug-Nutrient screen identifies bacterial effectors of metformin therapy. Cell 178: 1299-1312.e29, 2019.
10. Shen CL, Kaur G, Wanders D, Sharma S, Tomison MD, Ramalingam L, Chung E, Moustaid-Moussa N, Mo H and Dufour JM: Annatto-extracted tocotrienols improve glucose homeostasis and bone properties in high-fat diet-induced type 2 diabetic mice by decreasing the inflammatory response. Sci Rep 8: 11377, 2018.
11. Rahimi G, Heydari S, Rahimi B, Abedpoor N, Niktab I, Safaeinejad Z, Peymani M, Seyed Forootan F, Derakhshan Z, Esfahani MHN and Ghaedi K: A combination of herbal compound (SPTC) along with exercise or metformin more efficiently alleviated diabetic complications through down-regulation of stress oxidative pathway upon activating Nrf2-Keap1 axis in AGE rich diet-induced type 2 diabetic mice. Nutr Metab (Lond) 18: 14, 2021.
12. Satapati S, Kucejova B, Duarte JA, Fletcher JA, Reynolds L, Sunny NE, He T, Nair LA, Livingston KA, Fu X, *et al*: Mitochondrial metabolism mediates oxidative stress and inflammation in fatty liver. J Clin Invest 125: 4447-4462, 2015.
13. Tremblay BP and Haynes CM: Mitochondrial distress call moves to the cytosol to trigger a response to stress. Nature 579: 348-349, 2020.
14. Jing X, Du T, Chen K, Guo J, Xiang W, Yao X, Sun K, Ye Y, Guo F: Icariin protects against iron overload-induced bone loss via suppressing oxidative stress. Journal of cellular physiology 234: 10123-10137, 2019.
15. Liu S, Su Y, Sun B, Hao R, Pan S, Gao X, Dong X, Ismail AM and Han B: Luteolin protects against CIRI, potentially via regulation of the SIRT3/AMPK/mTOR signaling pathway. Neurochem Res 45: 2499-2515, 2020.
16. Li M, Wu C, Muhammad JS, Yan D, Tsuneyama K, Hatta H, Cui ZG and Inadera H: Melatonin sensitises shikonin-induced cancer cell death mediated by oxidative stress via inhibition of the SIRT3/SOD2-AKT pathway. Redox Biol 36: 101632, 2020.
17. Kim HS, Patel K, Muldoon-Jacobs K, Bisht KS, Aykin-Burns N, Pennington JD, van der Meer R, Nguyen P, Savage J, Owens KM, *et al*: SIRT3 is a mitochondria-localized tumor suppressor required for maintenance of mitochondrial integrity and metabolism during stress. Cancer Cell 17: 41-52, 2010.
18. Li P, Mao WW, Zhang S, Zhang L, Chen ZR and Lu ZD: Sodium hydrosulfide alleviates dexamethasone-induced cell senescence and dysfunction through targeting the miR-22/sirt1 pathway in osteoblastic MC3T3-E1 cells. Exp Ther Med 21: 238, 2021.
19. Hu J, Su B, Li X, Li Y and Zhao J: Klotho overexpression suppresses apoptosis by regulating the Hsp70/Akt/Bad pathway in H9c2(2-1) cells. Exp Ther Med 21: 486, 2021.
20. Fathi E, Valipour B, Sanaat Z, Nozad Charoudeh H and Farahzadi R: Interleukin-6, -8, and TGF-β secreted from mesenchymal stem cells show functional Role in reduction of telomerase activity of leukemia cell via Wnt5a/β-catenin and P53 pathways. Adv Pharm Bull 10: 307-314, 2020.
21. Fathi E, Farahzadi R, Javanmardi S and Vietor I: L-carnitine extends the telomere length of the cardiac differentiated CD117(+)-expressing stem cells. Tissue Cell 67: 101429, 2020.
22. Saha PC, Bera T, Chatterjee T, Samanta J, Sengupta A, Bhattacharyya M and Guha S: Supramolecular dipeptide-based near-infrared fluorescent nanotubes for cellular mitochondria targeted imaging and early apoptosis. Bioconjug Chem 32: 833-841, 2021.
23. Wang Y, Zeng G and Jiang Y: The emerging roles of miR-125b in cancers. Cancer Manag Res 12: 1079-1088, 2020.
24. Sim IW, Borromeo GL, Tsao C, Hardiman R, Hofman MS, Papatziamos Hjelle C, Siddique M, Cook GJR, Seymour JF and Ebeling PR: Teriparatide promotes bone healing in medication-related osteonecrosis of the jaw: A placebo-controlled, randomized trial. J Clin Oncol 38: 2971-2980, 2020.
25. Oryan A, Sahvieh S: Effects of bisphosphonates on osteoporosis: Focus on zoledronate. Life Sci 264: 118681, 2020.
26. Vatner SF, Zhang J, Oydanich M, Berkman T, Naftalovich R and Vatner DE: Healthful aging mediated by inhibition of oxidative stress. Ageing Res Rev 64: 101194, 2020.
27. Park JS, Piao J, Park G and Hong HS: Substance-P restores cellular activity of ADSC impaired by oxidative stress. Antioxidants (Basel) 9: 978, 2020.
28. Krishnaswamy VKD, Alugoju P and Periyasamy L: Effect of short-term oral supplementation of crocin on age-related oxidative stress, cholinergic, and mitochondrial dysfunction in rat cerebral cortex. Life sciences 263: 118545, 2020.
29. Sack MN, Rader DJ and Cannon RO III: Oestrogen and inhibition of oxidation of low-density lipoproteins in postmenopausal women. Lancet 343: 269-270, 1994.
30. Kushi LH, Folsom AR, Prineas RJ, Mink PJ, Wu Y and Bostick RM: Dietary antioxidant vitamins and death from coronary heart disease in postmenopausal women. N Engl J Med 334: 1156-1162, 1996.
31. Khaled S, Makled MN and Nader MA: Tiron protects against nicotine-induced lung and liver injury through antioxidant and anti-inflammatory actions in rats in vivo. Life Sci 260: 118426, 2020.
32. Luo X, Gong X, Su L, Lin H, Yang Z, Yan X and Gao J: Activatable mitochondria-targeting organoarsenic prodrugs for bioenergetic cancer therapy. Angew Chem Int Ed Engl 60: 1403-1410, 2021.
33. Houtkooper RH, Pirinen E, Auwerx J: Sirtuins as regulators of metabolism and healthspan. Nat Rev Mol Cell Biol 13: 225-238, 2012.
34. Yang W, Nagasawa K, Münch C, Xu Y, Satterstrom K, Jeong S, Hayes SD, Jedrychowski MP, Vyas FS, Zaganjor E, *et al*: Mitochondrial sirtuin network reveals dynamic SIRT3-dependent deacetylation in response to membrane depolarization. Cell 167: 985-1000.e21, 2016.

35. Hirschey MD, Shimazu T, Goetzman E, Jing E, Schwer B, Lombard DB, Grueter CA, Harris C, Biddinger S, Ilkayeva OR, *et al*: SIRT3 regulates mitochondrial fatty-acid oxidation by reversible enzyme deacetylation. Nature 464: 121-125, 2010.
36. Zhang DY, Gao T, Xu RJ, Sun L, Zhang CF, Bai L, Chen W, Liu KY, Zhou Y, Jiao X, *et al*: SIRT3 transfection of aged human bone marrow-derived mesenchymal stem cells improves cell therapy-mediated myocardial repair. Rejuvenation Res 23: 453-464, 2020.
37. Perović A, Sobočanec S, Dabelić S, Balog T and Dumić J: Effect of scuba diving on the oxidant/antioxidant status, SIRT1 and SIRT3 expression in recreational divers after a winter nondive period. Free Radic Res 52: 188-197, 2018.
38. Jehan S, Zhong C, Li G, Zulqarnain Bakhtiar S, Li D and Sui G: Thymoquinone selectively induces hepatocellular carcinoma cell apoptosis in synergism with clinical therapeutics and dependence of p53 status. Front Pharmacol 11: 555283, 2020.
39. Schumacker PT: A tumor suppressor SIRTainty. Cancer Cell 17: 5-6, 2010.
40. Govindarajulu M, Ramesh S, Neel L, Fabbrini M, Buabeid M, Fujihashi A, Dwyer D, Lynd T, Shah K, Mohanakumar KP, *et al*: Nutraceutical based SIRT3 activators as therapeutic targets in Alzheimer's disease. Neurochem Int 144: 104958, 2021.
41. Shukla S, Sharma A, Pandey VK, Raisuddin S and Kakkar P: Concurrent acetylation of FoxO1/3a and p53 due to sirtuins inhibition elicit Bim/PUMA mediated mitochondrial dysfunction and apoptosis in berberine-treated HepG2 cells. Toxicol Appl Pharmacol 291: 70-83, 2016.
42. Ghribi O, Herman MM, Spaulding NK and Savory J: Lithium inhibits aluminum-induced apoptosis in rabbit hippocampus, by preventing cytochrome c translocation, Bcl-2 decrease, Bax elevation and caspase-3 activation. J Neurochem 82: 137-145, 2002.
43. Zhou W, Liu Y, Shen J, Yu B, Bai J, Lin J, Guo X, Sun H, Chen Z, Yang H, *et al*: Melatonin increases bone mass around the prostheses of OVX rats by ameliorating mitochondrial oxidative stress via the SIRT3/SOD2 signaling pathway. Oxid Med Cell Longev 2019: 4019619, 2019.
44. Chiu HC, Chiu CY, Yang RS, Chan DC, Liu SH and Chiang CK: Preventing muscle wasting by osteoporosis drug alendronate in vitro and in myopathy models via sirtuin-3 down-regulation. J Cachexia Sarcopenia Muscle 9: 585-602, 2018.
45. Schurman L, McCarthy AD, Sedlinsky C, Gangoiti MV, Arnol V, Bruzzone L and Cortizo AM: Metformin reverts deleterious effects of advanced glycation end-products (AGEs) on osteoblastic cells. Exp Clin Endocrinol Diabetes 116: 333-340, 2008.
46. Wang L, Shi W, Gao X, SreeHarsha N and Zhang D: Cardioprotective role of metformin against sodium arsenite-induced oxidative stress, inflammation, and apoptosis. IUBMB Life 72: 749-757, 2020.
47. Rachner TD, Khosla S and Hofbauer LC: Osteoporosis: Now and the future. Lancet 377: 1276-1287, 2011.
48. Styrkarsdottir U, Cazier JB, Kong A, Rolfsson O, Larsen H, Bjarnadottir E, Johannsdottir VD, Sigurdardottir MS, Bagger Y, Christiansen C, *et al*: Linkage of osteoporosis to chromosome 20p12 and association to BMP2. PLoS Biol 1: E69, 2003.